

Effect of Momentum Ratio on the Mixing Performance of Unlike Split Triplet Injectors

Y. D. Won,* Y. H. Cho,[†] S. W. Lee,* and W. S. Yoon[‡]
Yonsei University, Seoul 120-749, Republic of Korea

Experimental investigation of mixing and mixing-controlled combustion efficiencies for sprays formed by unlike impinging split triplet injector elements was carried out. The quality of mixing was checked by performing cold-flow tests with inert simulant liquids. Measurements of local mass and mixture ratio distributions were made for different injection configurations and different jet momentum ratios. Results show that the quality of macroscopic mixing can be effectively characterized by the jet momentum ratio. The unlike split triplet element with lateral fuel injection is superior in mixing to either unlike doublet or unlike split triplet elements with central fuel injection. Secondary impingement appears to play a significant role in the extent of mixing. Mixing characteristics of the unlike split triplet element and its contribution to the promotion of macroscopic mixing efficiencies are discussed in detail.

Nomenclature

C^*	= characteristic velocity, m/s
D	= orifice diameter, mm
L	= orifice length, mm
M_l	= local mass, kg
M_t	= total mass, kg
MR	= momentum ratio
m	= mass flow rate, kg/s; total number of samples, $(n_1 + n_2)$
mr	= local mixture ratio
N_R	= Rupe number
n_1	= number of samples where $\gamma < R$
n_2	= number of samples where $\gamma > R$
R	= input (injection) mixture ratio
V	= speed of injected jet, m/s
Γ	= local mixture ratio for n_2
γ	= local mixture ratio for n_1
η	= mixing or C^* efficiency
μ	= dynamic viscosity, Pa · s
ρ	= density, kg/m ³

Subscripts

F	= fuel
l	= local
mix	= mixing
O	= oxidizer
S	= simulant
t	= total
theo	= theoretical value

Introduction

MANY liquid bipropellant rocket injectors have spray elements incorporating the impingement of two or more liquid jets. These elements are composed of oxidizer and fuel liquid streams that impinge at a given angle at a prescribed distance from the injector face. Impact waves caused by jet impingement act primarily for breakup and mixing of the liquids. The liquid sheet is disintegrated intermittently, generating groups of drops, and propagates showing wavelike expansion from the point of impingement. Formation of a fanlike elliptical liquid sheet in the perpendicular direction to the plane of the impinging jets results. Here, dissipative exchange of jet momentum provides direct mechanical mixing, and most mixing and atomization take place in the immediate vicinity of the impingement point. The impingement process, properly controlled, aids in spatial distribution as well as atomization of the liquids. In addition, one can accomplish a macroscopic mixing within the individual element's spray pattern. The dependability of the impinging element has been demonstrated in diverse applications such as numerous storable-propellant engines and small reaction control engines. Also the relative ease of fabrication of impinging elements makes this type of injector an attractive alternative to coaxial injector elements.¹

The spray characteristics of impinging injections were extensively studied in the late 1950s through the early 1960s.^{2–4} Numerous reports regarding spray characteristics, for example, drop size and velocity distribution, were issued. Heidmann et al.² conducted an extensive study of impinging jets to investigate the effects on spray characteristics of orifice diameter, jet velocity, impingement angle, preimpingement length, and liquid properties. Viscosity and surface tension effects were also investigated employing various types of simulants. Liquid jet velocity and impingement angle were noted to be main parameters controlling spray characteristics. Dombrowski and Hooper³ made cold-flow experimental efforts to investigate various aspects of jet impingement and spray formation. Photographs of sprays revealed that disintegration of the liquid sheet resulted from the formation of unstable waves of hydrodynamic origin. Both the disintegration of a sheet produced by impinging jets and the formation of droplets were shown to be principally dependent on jet flow properties and impingement angle. It was concluded that relative jet inertia is a controlling factor determining the spray pattern. Huang⁴ examined the breakup of axis symmetric liquid sheets by impinging two directly opposed water jets. Spray formation was classified into two dissimilar breakup regimes connected by a transition regime in terms of Weber number. George⁵ developed a correlation defining the relevance of the cold-flow data, such as drop sizes and impingement distance, to the hot firing results.

The analysis for impinging injection is not nearly as well developed as it is for coaxial injections, primarily due to insufficient

Received 11 April 2001; revision received 13 September 2001; accepted for publication 9 February 2002. Copyright © 2002 by the American Institute of Aeronautics and Astronautics, Inc. All rights reserved. Copies of this paper may be made for personal or internal use, on condition that the copier pay the \$10.00 per-copy fee to the Copyright Clearance Center, Inc., 222 Rosewood Drive, Danvers, MA 01923; include the code 0748-4658/02 \$10.00 in correspondence with the CCC.

*Graduate Student, Department of Mechanical Engineering, 134 Sinchon-Dong, Seodaemun-Gu; nicewyd@hanmail.net and lsw9394@hanmail.net.

[†]Graduate Student, Department of Mechanical Engineering, and Senior Research Engineer, Space Technology Research Department, HYUNDAI MOBIS and Graduate Student, 134 Sinchon-Dong, Seodaemun-Gu; yhcho@mobis.co.kr. AIAA Member.

[‡]Assistant Professor, School of Electrical and Mechanical Engineering, 134 Sinchon-Dong, Seodaemun-Gu; wsyoon@yonsei.ac.kr. AIAA Member.

information regarding fundamental mechanisms of spray formation, atomization, and mixing. Moreover, most of the previous studies of impinging injection focused on atomization, whereas rigorous studies of liquid-phase mixing are very limited. A summary of the initial studies of liquid/liquid-mixing characteristics for unlike impinging elements is presented in Ref. 6. These experiments involved changing the injector geometry and flow properties and recording the effects of these changes on the mixing quality. Empirical equations developed for the prediction of injection conditions for optimum mixing were similar for all unlike impinging patterns.⁶ Rupe conducted comprehensive experiments for the liquid-phase mixing by impinging nonreactive and immiscible simulant jets.⁷⁻¹⁰ In this series of measurements, mixing efficiency was examined with a variety of injector geometries and flow properties, and significant ranges of distinct variables for optimum mixing were suggested. Nurick and McHale¹¹ investigated the effect of orifice configuration on mixing characteristics. Occurrence of cavitation was also discussed in terms of orifice length/diameter ratio L/D . Sato¹² conducted atmospheric cold-flow tests with inert simulant liquids (trichloroethylene/water). The objective of these tests was to determine the cold-flow mass and mixture ratio distributions for use in the prediction of combustion efficiency. Agreement between the predicted values and the hot-fire test data was evident, which indicates that combustion is predominantly liquid-phase mixing controlled.

The ability to design unlike impinging elements to provide optimum spray distributions is contingent on having comprehensive design correlations that relate element mixing and atomization with injector geometric and hydraulic parameters. The primary objectives of the present study are the estimation of mixing performance, the investigation of the effect of momentum ratio on the mixing performance, and the extension of basic knowledge of liquid-phase mixing of an unlike split triplet element. Measurements of local mixture ratio distribution were made for different injection conditions and different momentum ratios (MRs). Nonreacting kerosene/water liquids simulate the kerosene/liquid oxygen (LOX) propellant combination. Mixing and mixing-controlled combustion efficiencies are discussed in terms of the jet MR.

Unlike Split Triplet Injector

The combustion chamber serves as an envelope to retain the propellants for a sufficient stay time to assure complete mixing and combustion before entering the nozzle. The volume of the combustion chamber, thus, has a definite effect on combustion efficiency, and the required chamber volume is a function of the stay time of propellant. To minimize the physical size of the combustion chamber, certain limitations have to be set on the stay time of the reactants in the chamber. Streaks due to highly stratified gas stream tubes are frequently observed.⁶ This specific physical evidence shows that the quality of reactant mixing and combustion are largely determined by liquid-phase mixing and corresponding initial liquid mass distribution. Gas-phase mixing appears to be less influential. The design of combustion, thus, requires sufficient knowledge of parameters controlling liquid-phase mixing.

Figure 1 shows the spray formations by unlike impinging elements. The liquid sheet after impingement continues to break up into droplets intermittently, and the resultant spray propagates while being dispersed or shatters into smaller drops. Impingement of liquid streams provides direct mechanical mixing and atomization, and numerous operational factors associated with jet impingement determine spray characteristics.⁶ Figure 1a shows the spray formation by an unlike doublet element with impingement angle of 60 deg, which is a representative design value for most unlike impinging injectors.⁶ Figure 1c shows the spray formation by an unlike split triplet element. This element is suitable for propellant combinations of higher mixture ratios. The configuration of jet impingement is similar to a conventional triplet impinger; the only difference is an additional center orifice on the split triplet for reducing the disparity between the fuel and oxidizer orifice sizes. A pair of parallel jets inside impinges on a pair of lateral jets injected at an included angle of 60 deg. Two successive impinging processes are incorporated in the spray formation by the unlike split triplet element. Two first

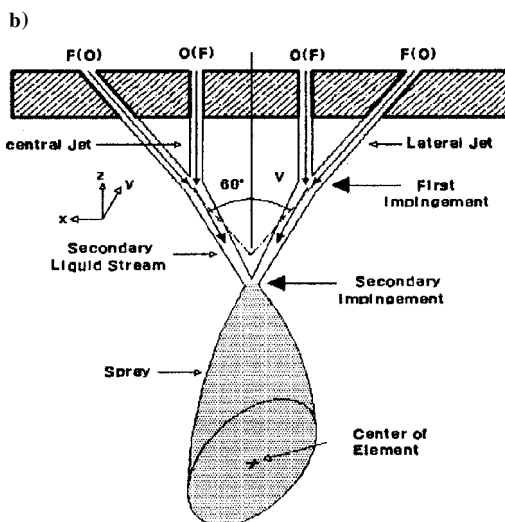
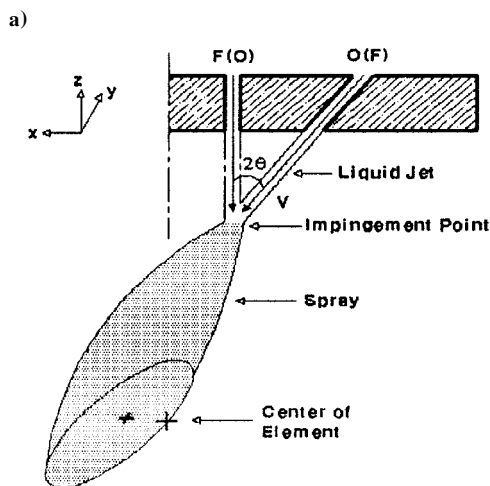
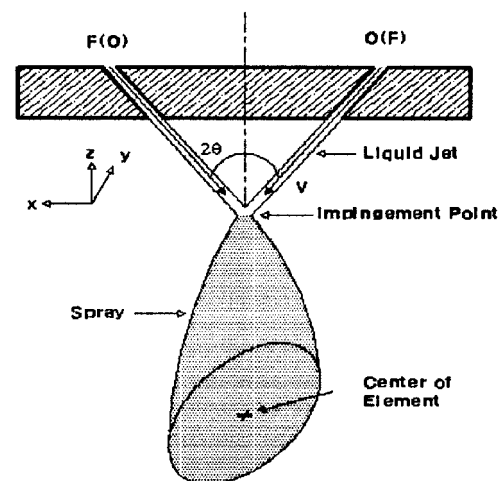


Fig. 1 Impinging jets and sprays: a) unlike doublet element ($2\theta = 60$ deg), b) unlike doublet element ($OF:2\theta = 30$ deg), and c) unlike split triplet element (FOOF or OFFO with included angle between lateral jets 60 deg).

impingements are made in unlike doublet fashion and generate a pair of secondary liquid streams (possibly in the form of spray, jets, or liquid sheets) (Fig. 1c). Higher impingement angles result in a higher impact-induced turbulence, hence higher turbulence mixing. Therefore, the quality of mixing after the first impingement with an impingement angle of 30 deg is expected to be lower than that by unlike doublet with an impingement angle of 60 deg. Stream-on-stream secondary impingement instead of coherent liquid jet impingement

is made at the second impingement point. Because flow properties of the two secondary liquid streams are identical, secondary impingement is carried out as in doublet fashion (Fig. 1c). The angle between the element's center axis and the resultant momentum vector of a spray is commonly defined as the beta angle.⁶ Because the maximum local mass flow shifts along the impinging plane in the direction of the high momentum stream, the vector of resultant spray is directed away from the central axis and the beta angle is always positive by definition (Fig. 1c). This always yields a longer secondary impingement height and a secondary impingement angle smaller than the included angle between the initial lateral jets. To explain the effect of the secondary impingement and its contribution on the promotion of macroscopic mixing quality, supplementary tests were conducted. Figure 1b shows the unlike doublet element with an impingement angle of 30 deg, which is identical to one-half of unlike split triplet elements (Fig. 1c). Hereinafter, referring to Fig. 1b, this unlike doublet element is oxidizer-fuel (OF) or fuel-oxidizer (FO) in accordance with the orifice arrangement. OF is an orifice array in which the oxidizer and fuel orifices are located sequentially from left, whereas FO is the reverse. Similarly, the orifice arrays of unlike split triplet injectors are fuel-oxidizer-oxidizer-fuel (FOOF) and oxidizer-fuel-fuel-oxidizer (OFFO) where FOOF and OFFO designate the array orifices from the left, respectively (Fig. 1c).

Experimental Apparatus and Procedure

A schematic of the test setup to measure the mass and the mixture ratio distributions is shown in Fig. 2. The system consists of sections of pressurization, regulation, and collection. Feeding and measuring circuits are typical where the nonreactive liquids are fed and collected.¹³ Advanced servocircuits were used to limit the fluctuation of pilot tank pressure, hence preventing fluctuations of liquid mass flow rates. A personal computer-based data acquisition system controls and records pressure, temperature, and mass flow rate. Recently, the authors conducted measurement of liquid-phase mixing with the use of optical devices.¹⁴ Detailed visualization of the local mixing process appears to be possible, theoretically at least. However, this rigorous method is less attractive due to its potential high cost and errors possibly involved in the multiple conversion processes of raw optic signals. Thus, the conventional patternation test method, in which the nonreactive simulant liquids are captured by a collector head and distributed to measuring cylinders, was adopted in the present study.

The spray was picked up by a 14 × 14 cm quadrilateral collector head, which is evenly divided into 400 (20 × 20) lattice cells. Fluid through each flow passage was collected by a transparent tube. Because the propellant simulants (water for oxidizer and kerosene for fuel) are immiscible, the volume of each of the two simulants collected at any given location is readily determined. The ratio of the

masses of each of the two liquids in a test cylinder represent the local mixture ratio. Spray was captured at a distance of 6.2 cm, where the spray is completely formed. Average collection efficiency was over 90%, considered to be sufficiently high for the estimation of mixing.¹²

Nonreactive storable simulants, water ($\rho_{S-O} = 1000 \text{ kg/m}^3$) for oxidizer and kerosene ($\rho_{S-F} = 807 \text{ kg/m}^3$) for fuel, simulate the real propellant combination. Water and kerosene were selected to provide dynamic similarities to the real propellant combination of LOX and kerosene. Density and viscosity of LOX are 1149 kg/m^3 ($\rho_{H_2O} = 1000 \text{ kg/m}^3$) and $1.9 \times 10^{-3} \text{ Pa} \cdot \text{s}$ ($\mu_{H_2O} = 1.005 \times 10^{-3} \text{ Pa} \cdot \text{s}$), respectively. The included angle between the two lateral jets was 60 deg for all injection elements. Orifice length/diameter ratio L/D was fixed at 6, which has been reported to be the minimum necessary to prevent the occurrence of cavitation.¹⁵ Fuel and oxidizer orifice diameters were all 0.4 mm, except for one case noted in Sec. IV in which the oxidizer orifice diameter was intentionally increased to examine the effect of orifice diameter ratio D_o/D_f on macroscopic mixing quality.

The flow characteristics of the liquid streams before impingement have significant effects on the mixing process. Even mixing and mixture ratio distributions, that is, optimum mixing, can be obtained at a certain impinging condition. This condition can be uniquely defined when flow properties of every liquid stream participating in the impingement are the same, and thus, the dynamic similarity between jets is perfect. This unique condition provides the baseline for the present study, and only the jet momentum is changed. The MRs of the jets were varied from 0.5 to 8.0 with jet Reynolds numbers in the range of 3×10^3 – 1.2×10^4 . The mechanism of liquid sheet disintegration is distinctly different depending on whether impinging liquid jets are laminar or turbulent.^{3,16} The liquid jet streams considered here are turbulent and dynamically similar. If the conditions under which the cold-flow data are obtained cause unique hydraulic flow characteristics, the relevance to hot firing results is questionable. To this end, additional hydraulic tests were conducted. The orifice discharge coefficients were measured to be between 0.8 and 0.9, and no unique hydraulic behavior was detected under all applied test conditions except the occurrence of cavitating bubbles in OFFO oxidizer streams when the jet velocity reaches its upper limit, $2\theta = 60 \text{ deg}$, $Re_o = 1.2 \times 10^4$.

Mixing and Characteristic Velocity Efficiencies

As mentioned earlier, combustion characteristics are largely determined by propellant spray distribution; thus, uniform liquid-phase mixing is essential for optimum combustion performance. The more thorough the mixing and the more uniform the distribution of the oxidizer relative to fuel, the more rapidly will the combustion products reach equilibrium composition. Although

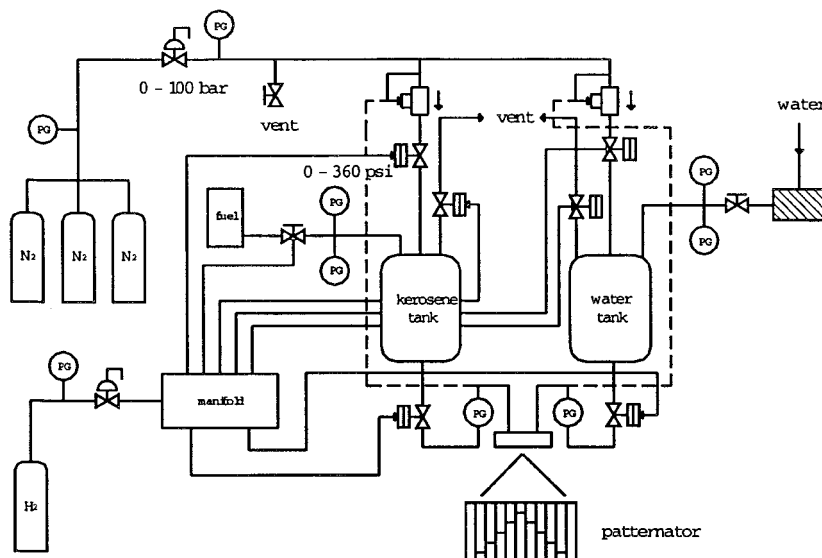


Fig. 2 Schematic of the patternation test facilities.

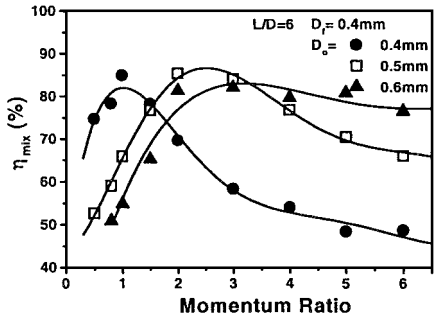
turbulence induced by combustion accounts for a major portion of the energy required for gas-phase mixing, thorough premixing of the liquid propellants must be accomplished by the injector if maximum performance is to be achieved.

The steps necessary to estimate mixing quality are 1) conduct patternator tests and measure the mixture fraction of each component in each test cylinder, 2) convert raw cold-flow data for real propellants, 3) arithmetically average local values weighted for mass fractions,

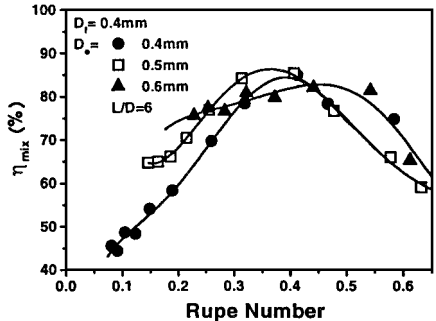
and 4) determine the extent of mixing. Heohn et al.¹⁷ defined the following mixing efficiency η_{mix} to describe the degree of mixing (percent) in the impinging injectors:

$$\eta_{\text{mix}} = 100 \times \left[1 - \left\{ \sum_1^{n_1} \frac{M_i \cdot (R - \gamma)}{M_i \cdot R} + \sum_1^{n_2} \frac{M_i \cdot (R - \Gamma)}{M_i \cdot (R - 1)} \right\} \right] \quad (1)$$

Mixing efficiency η_{mix} is based on the statistical variation in the local propellant mass fractions compared to the overall injected

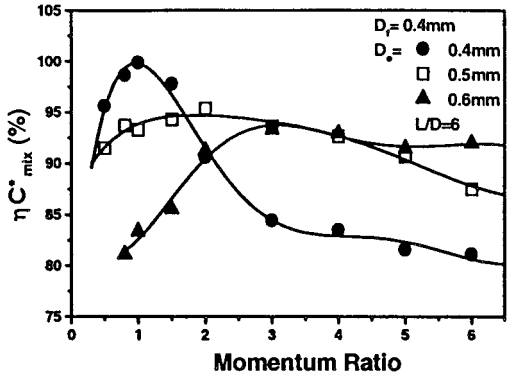


a) MR

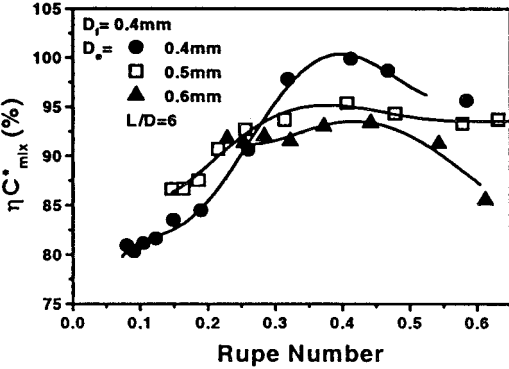


b) Rupe number

Fig. 3 Effect of diameter ratio on the mixing efficiency of unlike doublet element.

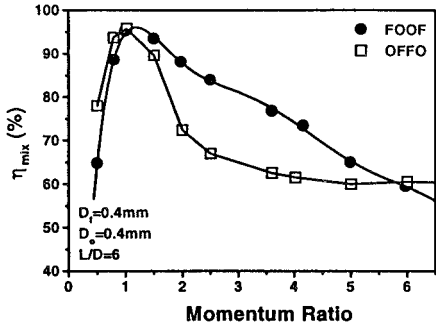


a) MR

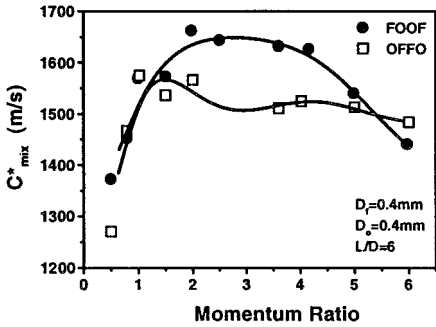


b) Rupe number

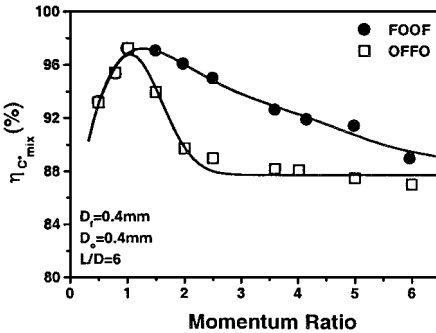
Fig. 4 Effect of diameter ratio on the characteristic velocity efficiency of unlike doublet element.



a) Mixing efficiency



b) Characteristic velocity



c) Characteristic velocity efficiency

Fig. 5 Mixing efficiencies of FOOF and OFFO split triplet elements vs MR.

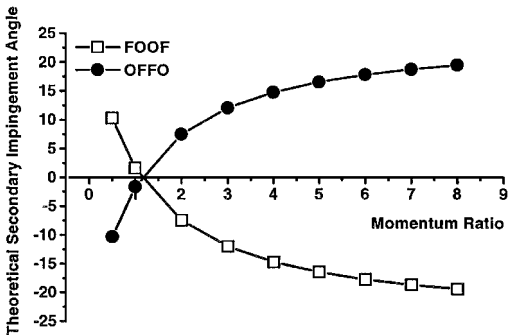


Fig. 6 Theoretical secondary impingement angle vs injection MR.

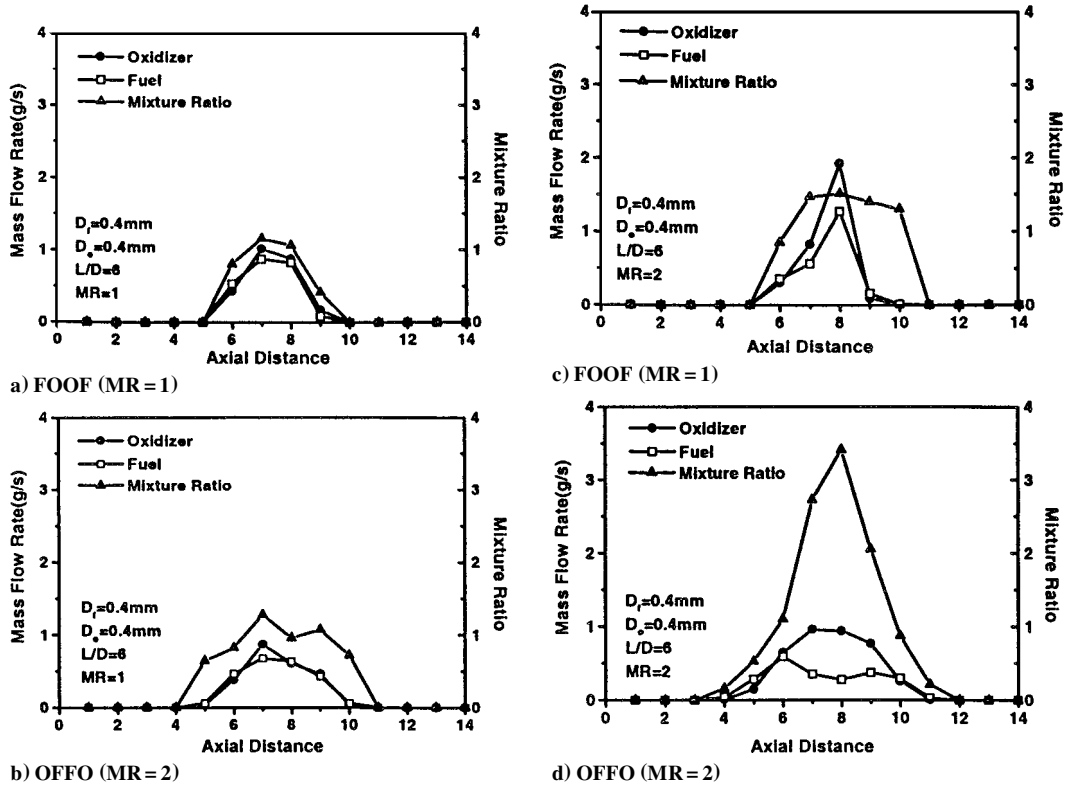


Fig. 7 Spatial variations of mass and mixture ratio along the perpendicular direction to the plane of impinging jets, with the momentum ratio of unity.

condition. It is a measure of the mixing on a macroscopic level as determined experimentally by a finite number of sampling cells, distributed on a collector head, intercepting the spray. As defined, this spray criterion may have any numerical value from 0 to 100 and represents all local values of the mixture ratio compared to the injection mixture ratio. When η_{mix} is 100, the mixture is everywhere uniform, at least at the macroscopic level, but if η_{mix} equals 0, the propellants are totally unmixed. Note that the propellant mixing of a uni-element injector is determined only by the intraelement mixing mechanism, as opposed to the combination of intra- and interelement mixing for a multi-element injector. Thus, a multi-element injector results in more uniform mixing than a uni-element injector across the entire chamber cross section.

A primary purpose of determining the mixing characteristics of bipropellant streams using the cold-flow technique is to gain confidence to predict injector hot firing performance, at least on a relative basis, assuming a known propellant vaporization rate. To this end, the mixing-controlled characteristic velocity (meters per second) and its efficiency (percent) are also calculated.

$$C_{\text{mix}}^* = \sum_{i=1}^m C_{\text{theo}, i}^* \cdot M_i / M_i \quad (2)$$

$$\eta_{C_{\text{mix}}^*} = 100 \times \frac{C_{\text{mix}}^*}{C_{\text{theo}}^*} \quad (3)$$

Mixing-controlled characteristic velocity C_{mix}^* , defined in Eq. (2), predicts injector hot firing performance.¹⁸ In Eq. (3) $\eta_{C_{\text{mix}}^*}$ is a direct measure of the loss of combustion performance due to incomplete mixing. In Eq. (3), C_{theo}^* is theoretical characteristic velocity, which is equivalent to combustion performance with perfect mixing, $\eta_{\text{mix}} = 100\%$.¹⁹ Note that, for simplicity, the definition of C_{mix}^* in Eq. (2) was made on the assumption that cold-flow mixing approximates real propellant mixing in the combustor environment.

MR as a Mixing Parameter

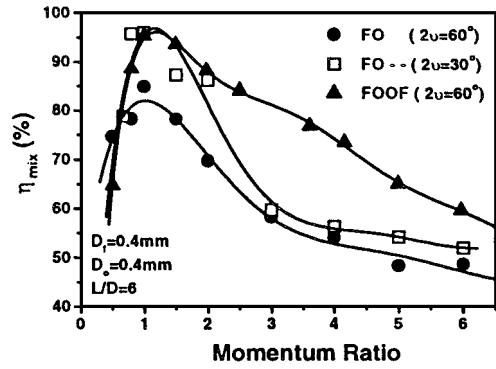
The mixing and mixing-controlled combustion efficiencies of the impinging injector can be represented in terms of several parameters

relevant to liquid jet velocity, such as mass ratio, MR, Rupe number, or even the velocity itself (see Ref. 18).

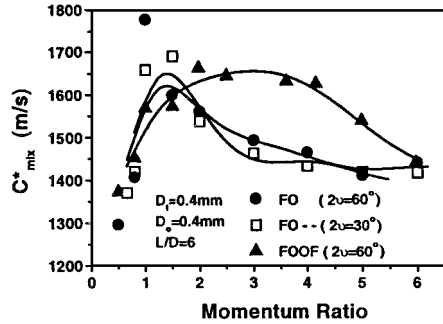
Rupe number N_R defines the fraction of the kinetic energy of one jet to the total kinetic energy of all jets $\{1/[1 + (\rho_F V_F^2 D_F)/(\rho_O V_O^2 D_O)]\}$ (Ref. 7). Rupe's criterion, has been used successfully by rocket engine manufacturers to optimize impinging injector design, and for this application it was emphasized that the impinging freestreams must be dynamically similar (fully developed turbulence preferred), symmetrical, and stable.²⁰ However, in practice, these conditions are hardly ever met due to operational requirements such as input propellant oxidizer/fuel (O/F) ratio or excess fuel supply for local thermal protection. With such specific requirements, effects of injector geometry and flow properties on the quality of mixing may not be clearly described by the Rupe number.

MR is defined simply as the ratio of the oxidizer jet momentum to fuel momentum $[(\rho_O V_O^2 D_O^2)/(\rho_F V_F^2 D_F^2)]$. When two or more jets impinge, liquid jets are broken up into droplets immediately in the vicinity of the impingement point. Spatial distributions of mass and mixture ratios are largely determined by the extent of penetration and corresponding momentum transfer (or exchange) by the liquid jet.²¹ As mentioned, disintegration of liquid sheets generally results from the formation of unstable waves of aerodynamic and hydrodynamic origin. At higher jet Reynolds numbers, the hydrodynamic impact waves due to momentum exchange are predominant over the whole liquid sheet, and exchange of jet momentum provides direct mechanical mixing. Therefore, the liquid jet MR is a useful mixing parameter for the prediction of combustion performance and stability.

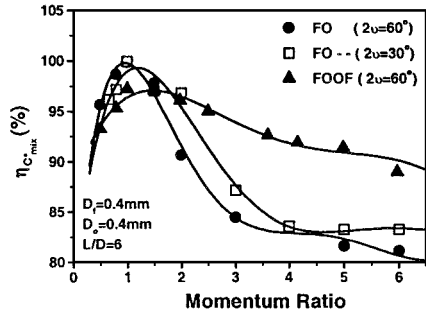
The η_{mix} mixing efficiency results for unlike doublet injection are plotted in Figs. 3a and 3b as a function of MR and Rupe number N_R , respectively. In these specific examples, the orifice diameter ratio is varied from unity to 1.25 and 1.5. In Fig. 3a, η_{mix} is maximum at the optimum MR of unity. Correlation of mixing for all unlike impinging elements shows optimum mixing when the jet momentum and the orifice diameters are equalized.^{2,6} In other words, all jets participating in the impingement must be the same in their momentum exchange, that is, in the extent of penetration, for uniform mixing. However, the diameter ratio for optimum mixing η_{mix} is



a) Mixing efficiency



b) Characteristic velocity

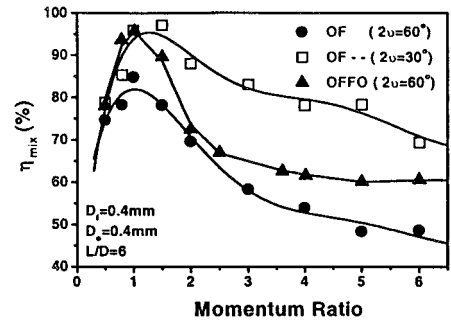


c) Characteristic velocity efficiency

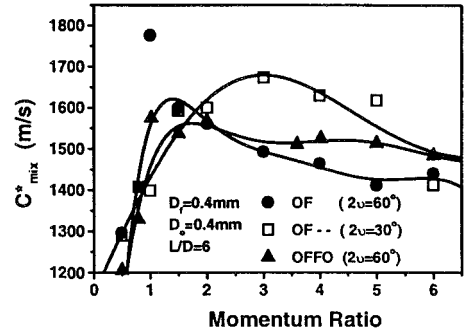
Fig. 8 Mixing efficiencies of FO unlike doublet and FOOF split triplet elements vs MR.

frequently not unity because most propellant combinations utilize larger oxidizer orifices to equalize fuel and oxidizer pressure drops. This dimensional disparity distorts the resulting spray shape and could impair mixing and atomization. Figure 3a shows the peaks shifting to high MRs as the diameter ratio increases over unity. The empirical correlation for diameter ratio⁶ shows that the optimum mixing is achieved at higher MR corresponding to the increase in diameter ratio. At fixed mass flow rate, jet momentum is inversely proportional to the orifice diameter, and an increase in oxidizer orifice diameter more greatly distorts the spray and degrades mixing with disparate deployment of fuel and oxidizer masses.³ In Fig. 3b, curves of mixing efficiencies in terms of Rupe number offer evidence of no consistent tendency associated with jet momentum and orifice diameter.

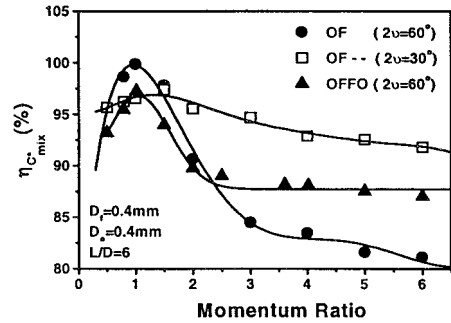
Figures 4a and 4b show characteristic velocity efficiencies as a function of MR and Rupe number, respectively. With increases in oxidizer orifice diameter, $\eta_{C^*_{mix}}$ curves are again shifted to a larger MR and their peak heights decrease consistently. As was mentioned earlier, the optimum mixing is achieved at higher MR corresponding to the increase in diameter ratio. However, the plot of $\eta_{C^*_{mix}}$ in terms of Rupe number in Fig. 4b does not properly show this common tendency: Peaks of $\eta_{C^*_{mix}}$ do not move in a certain direction as diameter ratio increases. It is presumed that such an inconsistent tendency is due to the definition of Rupe number. Therefore, throughout this study, the MR is used as an independent mixing parameter in the



a) Mixing efficiency



b) Characteristic velocity



c) Characteristic velocity efficiency

Fig. 9 Mixing efficiencies of OF unlike doublet and OFFO split triplet elements vs MR.

estimation of mixing and mixing-controlled combustion efficiencies of impinging elements.

Mixing Performance of the Split Triplet Impinging Injector

The mixing performance of FOOF and OFFO split triplet injector elements was investigated in terms of MR varied over a range of 0.5–8. The mixing efficiency η_{mix} , characteristic velocity C^*_{mix} , and characteristic velocity efficiencies $\eta_{C^*_{mix}}$ are plotted in Figs. 5a, 5b, and 5c, respectively. In all test cases, only the MR is changed by increasing the oxidizer jet momentum while maintaining unchanged the fuel jet momentum ($m_F = 1.98 \text{ g/s}$, $Re_F = 4,000$). Plots of η_{mix} and $\eta_{C^*_{mix}}$ all repeat the peaks occurring at the optimum momentum ratio of unity. As the MR approaches unity, the extent of penetration by both jets is equalized, and the state of mixing becomes optimum. Conditions for optimum mixing, such as an equal amount of horizontal momentum exchange and extent of penetration, are fulfilled at the MR of unity.

Mass distribution significantly changes with the MR, and any deviation from the MR of unity reduces the extent of mixing. Degradation of mixing is relatively more significant when the MR is less than unity ($MR < 1$). With higher momentum and penetration by the fuel jet, the vector of secondary liquid stream of FOOF is directed toward the central axis, whereas that of the secondary liquid stream of OFFO becomes farther away from the central axis. As the MR is increased above unity ($MR > 1$), penetration by the oxidizer

jet becomes superior. Fuel liquid stream is rapidly atomized and dispersed, but the oxidizer stream with higher initial momentum still preserves momentum sufficient to sustain itself as a coherent liquid stream and follows its own initial trajectory. Consequently, oxidizer fluids are more concentrated in the center of the spray field, whereas the fuel mass is more dispersed away from the center, resulting in the degradation of mixing.

The η_{mix} and $\eta_{C^*_{\text{mix}}}$ efficiencies of FOOF and OFFO unlike split elements are plotted in Figs. 5a and 5c, respectively. Here, both η_{mix} and $\eta_{C^*_{\text{mix}}}$ show markedly different tendencies between FOOF and OFFO. The η_{mix} mixing efficiencies of OFFO show a sharper decrease, whereas the degradation of FOOF mixing is more gradual. Proportionally increasing the velocity head of the FOOF oxidizer jet with the MR extends penetration into the fuel jet, and the vector of liquid stream formed by the first impingement is farther directed away from the central axis. This leads to degradation of atomization and mixing qualities (Fig. 5a). However, degradation is relatively less significant because additional secondary mixing compensates for the reduction of the mixing efficiency at the higher MR. Previous experimental studies revealed that, over a range of impingement angle from 40 to 80 deg, mixing increases as the impingement angle decreases.⁶ Decreasing of the secondary impingement angle of FOOF decreasing with the MR could be the reason for the improved efficiency. Figure 6 shows the angle between the element's center axis and the resultant momentum vector of a spray as a function of MR. The secondary liquid stream of OFFO is directed toward the central axis due to higher horizontal momentum. The velocity head of the OFFO oxidizer jet also further extends the penetration in accordance with the increase in MR, and the vector of secondary liquid stream is further directed toward the central axis. Secondary impingement is carried out in like-on-like fashion and ends up with the largest fraction of the oxidizer mass concentrated to the central axis, whereas fuel mass is dispersed around the periphery of the spray. Here, the augmentation of oxidizer jet momentum tends to increase the secondary impingement angle, and the secondary mixing with this enlarged secondary impingement angle is not more effective than FOOF. In the estimation of mixing qualities of injection elements, characteristic velocities must be considered because, after all, a rocket engine performance is based on its delivered C^* ,

not its C^* efficiency, which is theoretically only a function of the mixture ratio. Figure 5b shows very different C^*_{mix} curves with respect to each element and manifests the superiority of FOOF mixing. C^*_{mix} of FOOF is evenly distributed, less sensitive, and much higher than OFFO over a wide range of MR. For most practical propellant combinations, the oxidizer jet MR is higher than fuel jet. For instance, in the design of oxygen–hydrogen injectors, the value of the MR varies from 1.5 to 3.5 for liquid hydrogen injection. In the case of Unsymmetric Dimethyl Hydrazine/Nitrogen Tetroxide and RP-1/LOX propellant combinations, the heat release rate reaches maximum at the MR near 1.27 and 1.93, respectively, when the diameter ratio is unity.⁶ Conclusively, the FOOF element provides more flexibility to practical injector design because the degradation of mixing is relatively less significant over a wider range of MRs.

Figures 7a and 7b show fuel and oxidizer mass and mixture ratio distributions along a longer span of the spray fan when the MR is unity. With these optimum mixing conditions, the local mixture ratio of a larger number of cells was close to input mixture ratio and evenly distributed. This agrees with a previous result that the local mixture ratio along the major axis of the spray cross section is nearly constant and equal to the nominal value (if the spray is produced by streams of equal momentum and area ratios).⁷ Even with an MR of 2, mixture ratios of FOOF appear to be evenly distributed (Fig. 7c). However, for OFFO with a MR of 2 (Fig. 7d), oxidizer fluids are more concentrated in the center of the spray field, whereas the fuel mass is further dispersed away from the center. Consequently, the mixture ratio is very high at the central region of spray and drops rapidly as it moves away from the center. Degradation of mixing quality and poor mixing performance is apparent.

As is shown in Figs. 1b and 1c, configuration of unlike doublet injection with impingement angle of 30 deg is identical to one-half of a pair of first unlike doublet injections, due to the unlike split triplet element. FO (Fig. 8) and OF (Fig. 9), thus, exactly match for spray characteristics to those by the first unlike impingement of FOOF and OFFO, respectively. In Figs. 8 and 9, maximum efficiencies occur at the MR of unity again. It is apparent that, when $\text{MR} > 1$, mixing of FOOF is more effective than FO. Because the mixing condition of the first impingement of FOOF is exactly the

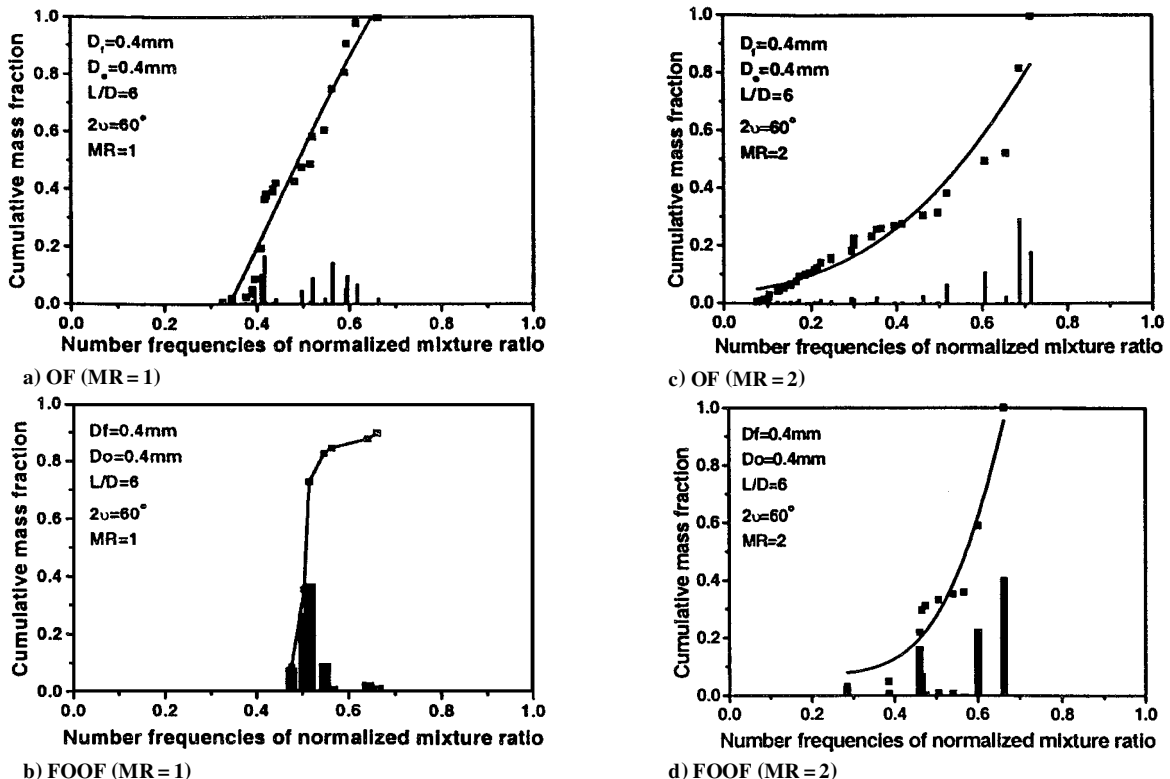


Fig. 10 Cumulative mass fraction vs. number frequencies of normalized mixture ratio when the MR is of unity.

same as FO, secondary impingement must be responsible for this difference. Contrary to FOOF, the secondary impingement of OFFO injection lowers the mixing quality (Fig. 9c). This tendency is confirmed from the plots of C_{mix}^* in Figs. 8b and 9b. C_{mix}^* of FOOF is evenly distributed and much higher than FOs as the MR is further increased over unity (Fig. 8b). On the contrary, the plot of OFFO C_{mix}^* in Fig. 9b is much lower than that of OF with the impingement angle of 30 deg. This verifies our previous result that the secondary impingement of OFFO degrades mixing at the higher MR.

Note that, in Figs. 8 and 9, the characteristic velocity efficiency is not always proportional to the mixing efficiency. This implies that, even with the assumption of mixing-controlled combustion, combustion efficiency cannot be predicted by the mixing efficiency only. This discrepancy is primarily because the homogeneity of the mixture ratio distribution was calculated by averaging local values in a linear and arithmetic manner, and the adiabatic flame temperature is inherently nonlinear against all thermodynamic properties. For instance, when the input mixture ratio is considerably different from stoichiometry, deviation of local values from input mixture ratio causes degradation of mixing. However, the thermodynamic relation may possibly predict a higher gas temperature if a given local mixture ratio is closer to stoichiometry. Thus, the averaged value of mass-weighted characteristic velocities may erroneously be larger than that arrived at from the input mixture ratio. This can bring about, in unique real situations, a characteristic velocity efficiency greater than 100%.²²

In the present study, it was assumed that qualities of liquid vaporization, gas-phase mixing, and chemical reaction are perfect and that combustion is controlled by the liquid-phase mixing only. However, the effect of atomization on mixing performance may be estimated in an indirect way. Consider one limiting situation in which all liquids are concentrated in one cell only and the opposite where liquids are evenly distributed in every cell on the collector head. In the former, the spray is simply the twofold result of the initial liquid jets, whereas in the latter, the spray completely covers the collector head with a uniform mixture ratio profile. In these two limiting situations, mixing and characteristic velocity efficiencies are erroneously the same ($\eta_{\text{mix}} = 100\%$), by definition [Eqs. (2) and (3)]. This specific example reveals that the profile of mixture ratio distribution must be considered simultaneously with the estimation of mixing quality.

Figure 10 shows cumulative mass in terms of the number frequency of the cells of a same mixture ratio. On the horizontal axis, local mixture ratios are normalized by the injection mixture ratio, and the vertical bar and solid square represent the sum of the local masses and the cumulative mass fraction to applicable mixture ratio, respectively. The steeper the slope is, the more uniform the mixture ratio distribution is. When the MR-1 (Figs. 10a and 10b) and 2 (Figs. 10c and 10d), it is commonly observed that curves of FOOF cumulative mass show more rapid growth than that of OF. FOOF with the MR of unity is noted to produce the most even distribution of mixture ratios and, thus, of uniform mixing.

Conclusions

Liquid-phase mixing caused by unlike split triplet impinging elements was studied experimentally. Measurements of local mass and mixture ratio distributions were made for different injection conditions and different momentum ratios. Nonreacting kerosene/water liquids simulate the kerosene/LOX propellant combination. Mixing and mixing-controlled combustion efficiencies were represented in terms of the O/F jet MR. General conclusions are as follows:

1) The quality of macroscopic mixing can be effectively characterized in terms of jet MR. Mixing is optimum at the MR of unity, and any deviation from the MR of unity causes degradation of mixing quality.

2) An FOOF split triplet element is superior to either unlike doublet or OFFO split triplet element. Secondary impingement of FOOF increases the mixing efficiency, whereas that of OFFO decreases the mixing efficiency.

3) Mixing by split triplet elements increases as the secondary impingement angle decreases. The secondary impingement angle appears to play a significant role in the extent of mixing of split triplet elements. Investigation of the detailed mechanism of the secondary impingement and mixing remains as a future task.

4) Most propellants utilize larger orifices to equalize fuel and oxidizer pressure drops. Experiments will be expanded to examine the effect of orifice diameter ratio on the mixing quality of the split triplet element.

References

1. Claflin, S. E., and Volkman, J. C., "Oxygen/Hydrogen Micro-Orifice Impinging Injector Development for Modular Test Chambers," *Proceeding of Propulsion Engineering Research Center Fourth Annual Symposium*, Huntsville, AL, Sept. 1992, pp. 53–58.
2. Heidmann, M. F., Priem, R. J., and Humphrey, J. C., "A Study of Sprays Formed by Two Impinging Jets," NACA TN 3855, March 1957.
3. Dombrowski, N., and Hooper, P. C., "A Study of the Sprays Formed by Impinging Jets in Laminar and Turbulent Flow," *Journal of Fluid Mechanics*, Vol. 18, Pt. 3, 1963, pp. 392–400.
4. Huang, J. P., "The Break-up of Axisymmetric Liquid Sheets," *Journal of Fluid Mechanics*, Vol. 43, Pt. 2, 1970, pp. 305–319.
5. George, D. J., "Rocket Injector Hot Firing and Cold Flow Spray Fields," AIAA Paper 73-1192, Nov. 1973.
6. *Liquid Rocket Engine Injectors*, NASA Space Vehicle Design Criteria SP-8089, 1986.
7. Rupe, J. H., "The Liquid Phase Mixing of A Pair of Impinging Streams," Jet Propulsion Lab., JPL Progress Rept. 20-195, California Inst. of Technology, Pasadena, CA, Aug. 1953.
8. Rupe, J. H., "A Correlation between the Dynamic Properties of a Pair of Impinging Streams and the Uniformity of Mixture Ratio Distribution in the Resulting Spray," Jet Propulsion Lab., JPL Progress Rept. 20-209, California Inst. of Technology, Pasadena, CA, 1956.
9. Rupe, J. H., "Experimental Studies of the Hydrodynamics of Liquid Propellant Injector," Jet Propulsion Lab., External Publ. 388, California Inst. of Technology, Pasadena, CA, June 1957.
10. Rupe, J. H., "An Experimental Correlation of the Nonreactive Properties of Injection Schemes and Combustion Effects in a Liquid Propellant Rocket Engine," Jet Propulsion Lab., JPL TR 32-255, California Inst. of Technology, Pasadena, CA, July 1965.
11. Nurick, W. H., and McHale, R. M., "Noncircular Orifice Holes and Advanced Fabrication Techniques for Liquid Rocket Injectors, Phase I Final Report," NASA CR-108570, Rocketdyne Div. North American Rockwell Corp., Oct. 1940.
12. Sato, K., "A Study of N₂O₄/Amine Injector Elements Part 1. Cold Flow Test," National Aerospace Laboratory of Japan, Rept. TR-899, 1986, pp. 1–13.
13. Nurick, W. H., and Clapp, S. D., "An Experimental Technique for Measurement of Injector Spray Mixing," *Journal of Spacecraft and Rockets*, Vol. 6, No. 11, 1969, pp. 1312–1315.
14. Vassallo, P., and Ashgriz, N., "Effect of Flow Rate on the Spray Characteristics of Impinging Water Jet," *Journal of Propulsion and Power*, Vol. 8, No. 5, 1992, pp. 980–986.
15. Reibling, R. W., and Powell, W. B., "The Hydraulic Characteristics of Flow through Miniature Slot Orifices," Jet Propulsion Lab., TR 32-1397, California Inst. of Technology, Pasadena, CA, Sept. 1969.
16. Anderson, W. E., Ryan, H. M., Pal, S., and Santoro, R. J., "Fundamental Studies of Impinging Liquid Jets," AIAA Paper 92-0458, Jan. 1992.
17. Heohn, F. W., Rupe, J. H., and Sotter, J. G., "Liquid-Phase Mixing of Bipropellant Doublets," Jet Propulsion Lab., TR 32-1546, California Inst. of Technology, Pasadena, CA, April 1972.
18. Wrobel, J. R., "Some Effects of Gas Stratification on Choked Nozzle Flows," AIAA Paper 64-266, Washington, DC, 1964.
19. Gordon, S., and McBride, B. J., "Computer Program for Calculation of Complex Chemical Equilibrium Composition, Rocket Performance, Incident and Reflected Shocks and Chapman-Jouguet Detonations," NASA SP-273, 1971.
20. Heohn, F. W., Rupe, J. H., and Sotter, J. G., "Liquid-Phase Mixing of Bipropellant Doublets," Jet Propulsion Lab., JPL TR 32-1546, California Inst. of Technology, Pasadena, CA, 1972.
21. Powell, W. B., "ICRPG Liquid Propellant Thrust Chamber Performance Evaluation Methodology," *Journal of Spacecraft and Rockets*, Vol. 1, No. 1, 1970, pp. 597–599.
22. Trinh, H. P., "Liquid Methane/Oxygen Injector Study for Potential Future Mars Ascent Engines," AIAA Paper 2000-3119, July 2000.